DOI: 10.1002/ejic.200701063

$[Ta_3O_3]A$ (A = Li, Na, K) and $[Ta_3O_3]B[Ta_3O_3]$ (B = Ca, Sr, Ba): Sandwich-Type Complexes Containing $Ta_3O_3^-$ δ and π Double Aromatic Ligands

Si-Dian Li,*[a] Chang-Qing Miao,[a] and Jin-Chang Guo[a]

Keywords: Sandwich-type complexes / Aromatic Ligands / Geometrical structure / Electronic structure / Density functional theory

A density functional theory investigation on half-sandwich-type C_{3v} $[Ta_3O_3]A$ (A = Li, Na, K) and full-sandwich-type D_{3h} $[Ta_3O_3]B[Ta_3O_3]$ (B = Ca, Sr, Ba) complexes containing $Ta_3O_3^-$ δ and π double aromatic ligands was performed. The $Ta_3O_3^-$ units serve as robust inorganic ligands in both $[Ta_3O_3]A$ and $[Ta_3O_3]B[Ta_3O_3]$ complex series, which are mainly maintained by A^+–$[Ta_3O_3]^-$ or $[Ta_3O_3]^-$–B^{2+}–$[Ta_3O_3]^-$ ionic interactions. These novel complexes turn out to be strongly thermodynamically favored in the gas phases and may be targeted in future experiments to open a new area of coordination chemistry by introducing δ and π double aromatic ligands into complex systems.

Introduction

A δ bond localized between two Re atoms was first discovered in $K_2[Re_2Cl_8]\cdot 2H_2O$ in 1964,[1] and the concept has been developed since then to a new branch of chemistry involving multiple metal–metal bonds with bond orders greater than three.[2] A Cr_2 compound containing a quintuple bond ($\sigma^2\pi^4\delta^4$) between two Cr atoms was synthesized in 2005.[3] However, the first circularly delocalized three-center δ bond was observed for $Ta_3O_3^-$ (D_{3h}, $^1A_1'$) in 2007 in a joint photoelectron spectroscopy (PES) and density functional theory (DFT) study.[4] $Ta_3O_3^-$ was confirmed to possess δ and π double aromaticity originating from the in-phase overlap of the Ta 5d atomic orbitals perpendicular to the molecular plane. The d-orbital-based delocalized molecular orbitals (MOs) of free $Ta_3O_3^-$ have the "appearance" of the totally delocalized π bonding MOs of the well-known $C_3H_3^+$ (with two π electrons) and $C_5H_5^-$ (with six π electrons), raising the possibility of utilizing $Ta_3O_3^-$ units as double aromatic ligands (δ and π) in sandwich-type complexes. This forms the objective to be achieved in this work at the DFT level. We focus our current research on half-sandwich-type C_{3v} $[Ta_3O_3]A$ (A = Li, Na, K) and full-sandwich-type D_{3h} $[Ta_3O_3]B[Ta_3O_3]$ (B = Ca, Sr, Ba), which all turned out to be true minima on the potential surfaces of the systems. The $Ta_3O_3^-$ units serve as robust inorganic ligands in these sandwich-type complexes, which are mainly maintained by A^+–$[Ta_3O_3]^-$ or $[Ta_3O_3]^-$–B^{2+}–$[Ta_3O_3]^-$ ionic interactions. Traditional sandwich-type complexes contain π aromatic ligands, exemplified by the prototypical $C_5H_5^-$ five-membered ring. The results obtained in this work provide the first sandwich-type complexes containing δ and π double aromatic ligands that are strongly energetically favored, and they may be targeted in future experiments to open a new area of coordination chemistry.

Computational Methodology

Structural optimizations, frequency analyses, and natural bond orbital (NBO) analyses were performed by using the Gaussian 03 program[5] at the hybrid DFT-B3LYP level[6] with the Stuttgart relativistic small core basis set and effective core potential (Stuttgart RSC 1997 ECP)[7] augmented with 2f and 1g functions[8] on Ta, Stuttgart RSC 1997 ECP bases[7] on Sr and Ba, and the 6-311+G(3df) basis[5,9] on Li, Na, K, Ca, O, C, and H. Ultrafine integration grids and tight optimization criteria were utilized throughout the structural optimization processes.[4] The results obtained in this work reproduce the results reported for $Ta_3O_3^-$ in ref.[4]; the DFT-B3PW91 approach[10] proves to produce essentially the same results as B3LYP. To check the local ring-current effect of the $Ta_3O_3^-$ ligands when incorporated into complexes, the widely used nucleus independent chemical shifts (NICS)[11] were calculated with the ghost atom lying both 1.0 Å [NICS(1)] and 2.0 Å [NICS(2)] above the Ta_3 plane along the molecular axes. Figure 1 depicts the optimized structures of the half-sandwich-type C_{3v} $[Ta_3O_3]A$ (A = Li, Na, K) and full-sandwich-type D_{3h} $[Ta_3O_3]B[Ta_3O_3]$ (B = Ca, Sr, Ba) complexes compared with free

[a] Institute of Materials Science and Department of Chemistry, Xinzhou Teachers' University, Xinzhou 034000, Shanxi, P. R. China

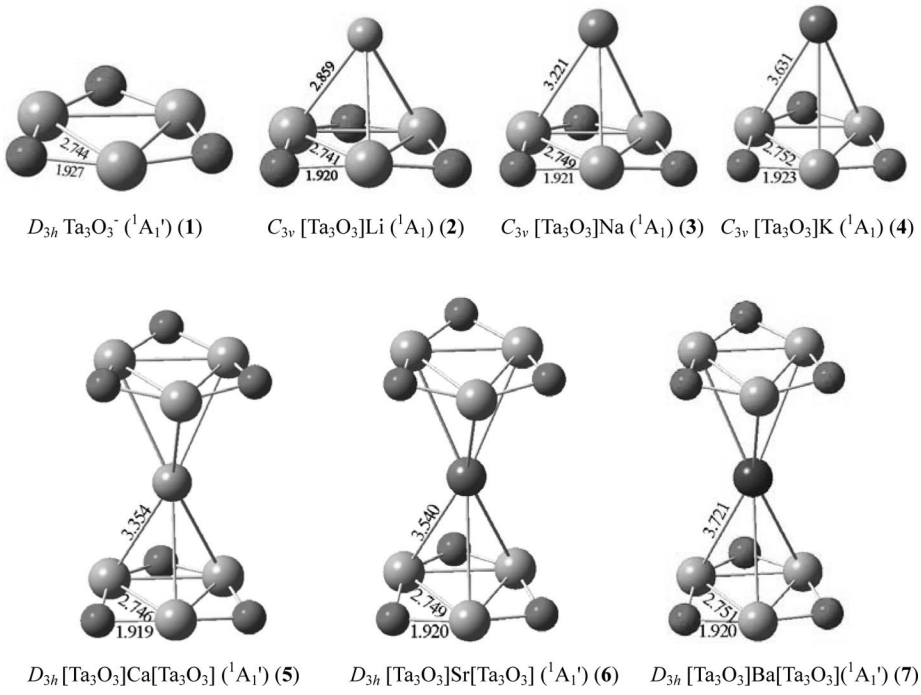

D_{3h} $Ta_3O_3^-$ ($^1A_1'$) (**1**) C_{3v} [Ta_3O_3]Li ($^1A_1$) (**2**) C_{3v} [Ta_3O_3]Na ($^1A_1$) (**3**) C_{3v} [Ta_3O_3]K ($^1A_1$) (**4**)

D_{3h} [Ta_3O_3]Ca[Ta_3O_3] ($^1A_1'$) (**5**) D_{3h} [Ta_3O_3]Sr[Ta_3O_3] ($^1A_1'$) (**6**) D_{3h} [Ta_3O_3]Ba[Ta_3O_3]($^1A_1'$) (**7**)

Figure 1. Optimized structures of C_{3v} [Ta_3O_3]A (A = Li, Na, K) and D_{3h} [Ta_3O_3]B[Ta_3O_3] (B = Ca, Sr, Ba) compared with free D_{3h} $Ta_3O_3^-$ at the DFT-B3LYP level with necessary bond lengths indicated in Å.

D_{3h} $Ta_3O_3^-$. These high-symmetry structures all proved to be true minima on their potential surfaces without imaginary frequencies, and they were well maintained when symmetry restrains were removed during structural optimizations. The mixed C_1 [Ta_3O_3]Ca[C_5H_5] and C_s [Ta_3O_3]Fe[C_5H_5] are compared in Figure 2. Figure 3 shows the top five occupied MOs of C_{3v} [Ta_3O_3]K and top ten MOs of D_{3h} [Ta_3O_3]Ca[Ta_3O_3], in comparison to the corresponding MOs of free D_{3h} $Ta_3O_3^-$.[4] Table 1 tabulates the calculated electronic properties and the lowest vibrational frequencies of the concerned complexes.

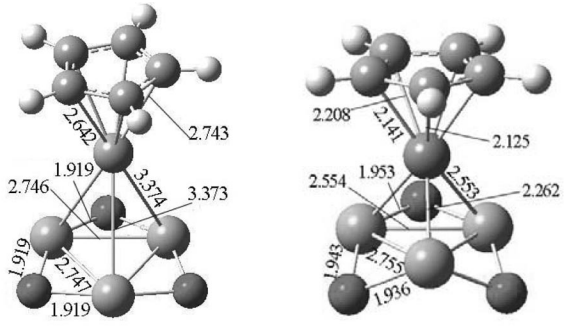

C_1 [Ta_3O_3]Ca[C_5H_5](^1A) (**8**) C_s [Ta_3O_3]Fe[C_5H_5]($^1A'$) (**9**)

Figure 2. Optimized structures of C_1 [Ta_3O_3]Ca[C_5H_5] and C_s [Ta_3O_3]Fe[C_5H_5] at the DFT-B3LYP level with important bond lengths indicated in Å.

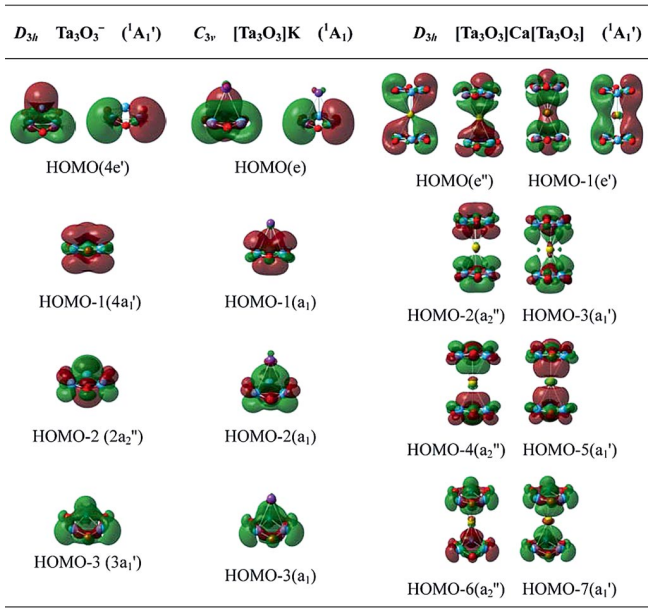

Figure 3. Top-five MOs of C_{3v} [Ta_3O_3]K and top-ten MOs of D_{3h} [Ta_3O_3]Ca[Ta_3O_3] compared with the top-five MOs of free D_{3h} $Ta_3O_3^-$.[4]

Table 1. Calculated HOMO energies E_{HOMO}, HOMO–LUMO energy gaps ΔE_{gap}, natural atomic charges of the metal centers A or B $q_{A/B}$, total Wiberg bond indices of A or B centers $WBI_{A/B}$, Wiberg bond indices of the Ta–Ta bond WBI_{Ta-Ta} and the Ta–O bond WBI_{Ta-O}, NICS(1) and NICS(2) values, and the lowest vibrational frequencies ν_{min} of C_{3v} $[Ta_3O_3]A$ (A = Li, Na, K), D_{3h} $[Ta_3O_3]B[Ta_3O_3]$, and C_1 $[Ta_3O_3]Ca[C_5H_5]$ at the B3LYP level. Free D_{3h} $Ta_3O_3^-$ is tabulated for comparison.

	E_{HOMO} [eV]	ΔE_{gap} [eV]	$q_{A/B}$ [|e|]	$WBI_{A/B}$	WBI_{Ta-Ta}	WBI_{Ta-O}	NICS(1)	NICS(2)	ν_{min} [cm^{-1}]
$Ta_3O_3^-$	–0.885	2.225			1.06	0.72	–48.8	–14.2	61
$(Ta_3O_3)Li$	–4.822	2.283	+0.68	0.56	1.10	0.75	–42.7	–11.6	102
$(Ta_3O_3)Na$	–4.604	2.220	+0.70	0.52	1.08	0.74	–38.2	–10.8	74
$(Ta_3O_3)K$	–4.342	2.233	+0.83	0.33	1.06	0.74	–40.5	–11.7	56
$(Ta_3O_3)Ca(Ta_3O_3)$	–5.012	2.182	+1.28	1.17	1.07	0.75	–43.8	–12.2	6
$(Ta_3O_3)Sr(Ta_3O_3)$	–5.019	2.230	+1.38	1.06	1.06	0.75	–43.1	–12.1	5
$(Ta_3O_3)Ba(Ta_3O_3)$	–4.911	2.142	+1.49	0.96	1.04	0.75	–45.2	–12.9	7
$(Ta_3O_3)Ca(C_5H_5)$	–5.111	2.282	+1.55	0.83	≈1.07	≈0.75	–41.5	–6.2	7

Results and Discussions

C_{3v} $[Ta_3O_3]A$ (A = Li, Na, K)

When one alkali metal cation A^+ (M^+ = Li^+, Na^+, K^+) approaches a free D_{3h} $Ta_3O_3^-$ (**1**) ion along the threefold molecular axis, the half-sandwich-type C_{3v} $[Ta_3O_3]A$ series is produced (**2**, **3**, **4** in Figure 1), and the bond lengths are r_{Ta-Ta} = 2.741, 2.749, 2.752 Å, r_{Ta-O} = 1.920, 1.921, 1.923 Å, and r_{Ta-A} = 2.859, 3.221, 3.631 Å for A = Li, Na, and K, respectively. Obviously, the $Ta_3O_3^-$ structural units were preserved in these half-sandwich-type complexes when compared to those in free D_{3h} $Ta_3O_3^-$. Table 1 indicates that Ta–Ta and Ta–O interactions are typical single bonds throughout the whole sandwich-type complex series, and Wiberg bond indices[12] of $WBI_{Ta-Ta} \approx 1.0$ and $WBI_{Ta-O} \approx 0.74$ were found. The A^+–$[Ta_3O_3]^-$ ionic interactions are clearly demonstrated by the fact that alkali atoms in these complexes possess high calculated natural atomic charges with q_{Li} = +0.68 |e|, q_{Na} = +0.70 |e|, and q_K = +0.83 |e|. The ionicity of these complexes increases from A = Li, Na, to K, in line with the corresponding total Wiberg bond indices, which decrease from WBI_{Li} = 0.56, WBI_{Na} = 0.52, to WBI_K = 0.33. The energy of the highest occupied molecular orbital (HOMO) of the system is effectively lowered from –0.885 eV in free $Ta_3O_3^-$ (**1**) to –4.822 eV in $[Ta_3O_3]Li$ (**2**), –4.604 eV in $[Ta_3O_3]Na$ (**3**), and –4.342 eV in $[Ta_3O_3]K$ (**4**), and the corresponding HOMO–LUMO energy gaps are greater than 2.22 eV. Table 1 indicates that the calculated NICS(1) (–38.2 to –42.7 ppm) and NICS(2) (–10.8 to –11.7 ppm) of these half-sandwich complexes are systematically lower than the corresponding values [NICS(1) = –48.8 ppm and NICS(2) = –14.2 ppm] of the free D_{3h} $Ta_3O_3^-$ ligand, which clearly provides evidence for the presence of a local ring-current effect on the Ta_3 triangles and therefore the aromatic nature of the $Ta_3O_3^-$ ligands in these novel complexes. NICS values vary with the locations of the ghost atoms.[11] The calculated NICS(2) values are close to the value of NICS(1) = –9.9 ppm calculated for $C_5H_5^-$ at the same theoretical level. Considering that fact that transition metals possess much bigger atomic sizes than carbon with expanded orbital distributions, we suggest that NICS(2) is a suitable aromatic indicator for transition-metal rings.

D_{3h} $[Ta_3O_3]B[Ta_3O_3]$ (B = Ca, Sr, Ba)

With two $Ta_3O_3^-$ ligands sandwiching one alkaline-earth metal dication (B^{2+}) from opposite ends along the threefold axis of the system, the eclipsed D_{3h} $[Ta_3O_3]B[Ta_3O_3]$ neutrals (B = Ca, Sr, Ba) were formed (**5**, **6**, **7**), whereas their staggered counterparts D_{3d} $[Ta_3O_3]B[Ta_3O_3]$ turned out to be transition states. For examples, D_{3h} $[Ta_3O_3]Ca[Ta_3O_3]$ is a true minimum with the lowest vibrational frequency of +6 cm^{-1} (a vibrational mode in which the two $Ta_3O_3^-$ ligands rotate in opposite directions along the threefold molecular axis), whereas D_{3d} $[Ta_3O_3]Ca[Ta_3O_3]$ proves to have an imaginary vibrational frequency of –6i cm^{-1}. The $D_{3d} \rightarrow D_{3h}$ rotatory transition for $[Ta_3O_3]Ca[Ta_3O_3]$ has a low energy barrier of 0.02 eV, similar to the $D_{5d} \rightarrow D_{5h}$ structural transition of the well-known $[C_5H_5]_2Fe$.[13,14] As shown in Figure 1 and Table 1, the $Ta_3O_3^-$ units in these D_{3h} sandwich-type complexes have also been well preserved, and the O atoms are only slightly off-planed and the Ta–Ta and Ta–O single bonds are well maintained. The alkaline-earth metal centers in these complexes are highly positively charged: q_{Ca} = +1.28 |e|, q_{Sr} = +1.38 |e|, and q_{Ba} = +1.49 |e|, which indicates that there is increasing ionicity in the $[Ta_3O_3]^-$–B^{2+}–$[Ta_3O_3]^-$ series from B = Ca, Sr, to Ba. These complexes also possess considerably negative HOMO energies (lower than –4.91 eV) and wide HOMO–LUMO energy gaps (greater than 2.14 eV). The calculated NICS(1) (–43.1 to –45.2 ppm) and NICS(2) (–12.1 to –12.9 ppm) values of these complexes are again in accord with the corresponding values of free D_{3h} $Ta_3O_3^-$, which indicates that the ring-current effect of the $Ta_3O_3^-$ ligands was also inherited in these full-sandwich-type complexes.

As outlined in Figure 2 and Table 1, a full-sandwich-type structure was obtained for the mixed C_1 $[Ta_3O_3]Ca[C_5H_5]$ (**8**), which is slightly distorted from C_s symmetry with two different ligands: one $Ta_3O_3^-$ and one $C_5H_5^-$ anion. Both ligands are preserved and form effective $[Ta_3O_3]^-$–Ca^{2+}–$[C_5H_5]^-$ ionic interactions. It should be pointed out that the local ring-current effect of the $Ta_3O_3^-$ ligand remains in **8**, as evidenced by its negative NICS values, which are comparable to the corresponding values of free $Ta_3O_3^-$ (see Table 1). However, when the Ca center is replaced with an Fe one, the resulting Fe-centered mixed C_s $[Ta_3O_3]Fe[C_5H_5]$ (**9**) complex is much different from **8**: the Fe center in **9**

forms two strong Fe–Ta covalent bonds (r_{Fe-Ta} = 2.26 Å) and one effective Fe–Ta covalent interaction (r_{Fe-Ta} = 2.55 Å) in the $[Ta_3O_3]Fe$ half, whereas the $Fe[C_5H_5]$ half possesses five Fe–C coordination interactions similar to that in ferrocene (**9** has the averaged Fe–C distance of r_{Fe-C} = 2.13 Å, which is slightly longer than the corresponding value of r_{Fe-C} = 2.064 Å in ferrocene).[13,14] MO analysis indicates that the delocalized δ and π MOs over the $Ta_3O_3^-$ ligand are severely weakened in **9** by the formation of three Fe–Ta covalent interactions. Complex **9** can be practically viewed as half coordinative and half covalent. Similar Fe–Ta covalent bonds exist in $[Ta_3O_3]Fe[Ta_3O_3]$. Because transition metals with partially filled $(n-1)$d orbitals are very different from the alkali and alkaline-earth metals, which have the lowest electronegativities in the periodic table and empty $(n-1)$d orbitals, they form effective d–d covalent bonds with the Ta_3 triangular ring in the Ta_3O_3 units and form transition-metal oxide clusters rather than sandwich-type complexes.

Molecular Orbital Analyses

MO analyses help to understand the bonding nature of these complexes. As clearly shown in Figure 3, the top five MOs of free D_{3h} $Ta_3O_3^-$[4] were essentially maintained in C_{3v} $[Ta_3O_3]K$ (**4**), as only slight distortions are observed, and the K center in $[Ta_3O_3]K$ is practically a naked cation. The calculated atomic configuration of $K[Ar]4s^{0.15}3d^{0.02}$ and the total Wiberg bond index of WBI_K = 0.33 support the ionic bonding nature of the K^+–$[Ta_3O_3]^-$ interaction. The K atom loses its $4s^1$ electron almost completely, whereas its 3d orbital remains practically empty in **4**. Similar results exist for $[Ta_3O_3]Li$ and $[Ta_3O_3]Na$. In $[Ta_3O_3]B[Ta_3O_3]$ full-sandwich-type complexes, alkaline-earth metal centers possess the natural atomic configurations of $Ca[Ar]4s^{0.53}3d^{0.17}$, $Sr[Kr]5s^{0.46}4d^{0.15}$, and $Ba[Xe]6s^{0.31}5d^{0.20}$, respectively. In these complexes, alkaline-earth metal centers lose most of their ns^2 electrons, whereas their $(n-1)$d orbitals gain only a small portion back from the $Ta_3O_3^-$ ligands (≤0.20 |e|). The low occupations of the valence $(n-1)$d atomic orbitals indicate that covalent d–d interactions only contribute slightly to the overall bonding of the systems, as also evidenced by the low Wiberg bond indices of WBI_{Ca-Ta} = 0.18, WBI_{Sr-Ta} = 0.16, and WBI_{Ba-Ta} = 0.15 (compare with ferrocene,[13,14] in which the Fe–C coordination bonds have bond orders of WBI_{Fe-C} = 0.29 at the B3LYP level). As shown in Figure 3, the degenerate HOMO(e″) and degenerate HOMO-1(e′) of the D_{3h} $[Ta_3O_3]Ca[Ta_3O_3]$ (**5**) mainly originate from the two degenerate HOMO(4e′) of free $Ta_3O_3^-$ with only slight contributions from the Ca $4d_{xz}$ (or $4d_{yz}$) atomic orbitals [which partially participate in the HOMO(e″)]. More interestingly, the HOMO-2(a_2'') and HOMO-3(a_1') of **5** inherit the MO features of the delocalized δ HOMO-1(4a′) of free $Ta_3O_3^-$, whereas its HOMO-4(a_2'') and HOMO-5(a_1') mainly originate from the delocalized π HOMO-2($2a_2''$) of the ligands. It is these delocalized δ and π MOs that render local ring-current effects to the Ta_3 triangles, which therefore doubles the aromaticity of the $Ta_3O_3^-$ ligands in these sandwich-type complexes. HOMO-6(a_2'') and HOMO-7(a_1') of $[Ta_3O_3]Ca[Ta_3O_3]$ can be clearly traced back to the complete σ bonding HOMO-3($3a_1'$) of $Ta_3O_3^-$. Other inner-shell valence MOs are mainly responsible for the polarized Ta–O interactions or pure oxygen lone pairs within the ligands.[4]

Thermodynamic Stabilities

Concerning the thermodynamic stabilities of these complexes, we calculated the energy changes of the following processes in the gas phases starting from the experimentally known $Ta_3O_3^-$ anions[4] and alkali (A^+) or alkaline-earth-metal (B^{2+}) cations to the required neutral complexes [Equations (1) and (2)]:

$$Ta_3O_3^- (D_{3h}) + A^+ = [Ta_3O_3]A\ (C_{3v}) \quad (1)$$

$$2Ta_3O_3^- (D_{3h}) + B^{2+} = [Ta_3O_3]B[Ta_3O_3]\ (D_{3h}) \quad (2)$$

With zero-point corrections included, Equation (1) has the energy changes of $\Delta E(1)$ = –570, –493, and –410 kJ/mol for A = Li, Na, and K, respectively, and Equation (2) possesses the energy changes of $\Delta E(2)$ = –1769, –1623, and –1501 kJ/mol for B = Ca, Sr, and Ba, respectively. For the mixed C_1 $[Ta_3O_3]Ca[C_5H_5]$, ΔE = –1913 kJ/mol. These huge negative energy changes indicate that the $[Ta_3O_3]A$ (C_{3v}), $[Ta_3O_3]B[Ta_3O_3]$ (D_{3h}), and $[Ta_3O_3]Ca[C_5H_5]$ complexes are strongly favored over ionic dissociations in the gas phase, and they are therefore viable in experiments. Replacement of $Ta_3O_3^-$, A^+, and B^{2+} in Equations (1) and (2) with Ta_3O_3 (which has a C_1 symmetry slightly distorted from D_{3h}) and A and B neutrals, respectively, produces the corresponding values of $\Delta E(1)$ = –228, –170, and –177 kJ/mol and $\Delta E(2)$ = –410, –388, and –422 kJ/mol, respectively. These negative energy changes further indicate that Equations (1) and (2) are also favored over covalent dissociations. A detailed molecular dynamic study of these processes is beyond the reach of available computing resources at the current stage.

Conclusions

We presented a DFT investigation on the half-sandwich-type C_{3v} $[Ta_3O_3]A$ (A = Li, Na, K) and full-sandwich-type D_{3h} $[Ta_3O_3]B[Ta_3O_3]$ (B = Ca, Sr, Ba) complexes containing $Ta_3O_3^-$ δ and π double aromatic ligands. These sandwich-type complexes are mainly maintained by ionic interactions due to the fact that both alkali (A) and alkaline-earth (B) metals have the lowest electronegativities in the periodic table; the $Ta_3O_3^-$ anions serve as robust inorganic ligands in these complexes. Modification to the $Ta_3O_3^-$ ligands or substitution of Ta with other low-oxidation-state transition metals may produce various derivatives. Preliminary investigations have shown that both $Nb_3O_3^-$ and $V_3O_3^-$ anions form similar sandwich-type complexes. These model complexes are strongly favored in energy and could be targeted

in future experiments to open a new area of coordination chemistry by introducing δ and π double aromatic ligands to complex systems.

Acknowledgments

The authors sincerely thank the joint financial support of the Natural Science Foundation of China (No. 20573088) and Shanxi Natural Science Foundation (No. 2006011024).

[1] F. A. Cotton, N. F. Curtis, C. B. Harris, B. F. G. Johnson, S. J. Lippard, J. T. Mague, W. R. Robinson, J. S. Wood, *Science* **1964**, *145*, 1305.
[2] F. A. Cotton, C. A. Murillo, R. A. Walton, *Multiple Bonds Between Metal Atoms*, 3rd ed., Springer, New York, **2005**.
[3] T. Nguyen, A. D. Sutton, M. Brynda, J. C. Fettiger, G. J. Long, P. P. Power, *Science* **2005**, *310*, 844.
[4] H.-J. Zhai, B. B. Averkiev, D. Y. Zubarev, L.-S. Wang, A. I. Boldyrev, *Angew. Chem. Int. Ed.* **2007**, *46*, 4277.
[5] M. J. Frisch, G. W. Trucks, H. B. Schlegel, G. E. Scuseria, M. A. Robb, J. R. Cheeseman, J. A. Montgomery Jr, T. Vreven, K. N. Kudin, J. C. Burant, J. M. Millam, S. S. Iyengar, J. Tomasi, V. Barone, B. Mennucci, M. Cossi, G. Scalmani, N. Rega, G. A. Petersson, H. Nakatsuji, M. Hada, M. Ehara, K. Toyota, R. Fukuda, J. Hasegawa, M. Ishida, T. Nakajima, Y. Honda, O. Kitao, H. Nakai, M. Klene, X. Li, J. E. Knox, H. P. Hratchian, J. B. Cross, C. Adamo, J. Jaramillo, R. Gomperts, R. E. Stratmann, O. Yazyev, A. J. Austin, R. Cammi, C. Pomelli, J. W. Ochterski, P. Y. Ayala, K. Morokuma, G. A. Voth, P. Salvador, J. J. Dannenberg, V. G. Zakrzewski, S. Dapprich, A. D. Daniels, M. C. Strain, O. Farkas, D. K. Malick, A. D. Rabuck, K. Raghavachari, J. B. Foresman, J. V. Ortiz, Q. Cui, A. G. Baboul, S. Clifford, J. Cioslowski, B. B. Stefanov, G. Liu, A. Liashenko, P. Piskorz, I. Komaromi, R. L. Martin, D. J. Fox, T. Keith, M. A. Al-Laham, C. Y. Peng, A. Nanayakkara, M. Challacombe, P. M. W. Gill, B. Johnson, W. Chen, M. W. Wong, C. Gonzalez, J. A. Pople, *Gaussian 03*, Revision B.03, Gaussian, Inc., Pittsburgh, **2003**.
[6] a) A. D. Becke, *J. Chem. Phys.* **1993**, *98*, 5648; b) C. Lee, W. Yang, R. G. Parr, *Phys. Rev. B* **1988**, *37*, 785; c) B. Miehlich, A. Savin, H. Stoll, H. Preuss, *Chem. Phys. Lett.* **1989**, *157*, 200.
[7] Stuttgart RSC 1997 ECP basis sets used in this work and the related references therein can be obtained from https://bse.pnl.gov/bse/portal.
[8] J. M. L. Martin, A. Sundermann, *J. Chem. Phys.* **2001**, *114*, 3408.
[9] a) A. D. McLean, G. S. Chandler, *J. Chem. Phys.* **1980**, *72*, 5639; b) R. Krishnan, J. S. Binkley, R. Seeger, J. A. Pople, *J. Chem. Phys.* **1980**, *72*, 650; c) J.-P. Blaudeau, M. P. McGrath, L. A. Curtiss, L. Radom, *J. Chem. Phys.* **1997**, *107*, 5016; d) T. Clark, J. Chandrasekhar, G. W. Spitznagel, P. v. R. Schleyer, *J. Comput. Chem.* **1983**, *4*, 294.
[10] K. Burke, J. P. Perdew, Y. Wang in *Electronic Density Functional Theory: Recent Progress and New Directions* (Eds.: J. F. Dobson, G. Vignale, M. P. Das), Plenum, **1998**.
[11] a) P. v. R. Schleyer, C. Maerker, A. Dransfeld, H. J. Jiao, N. Hommes, *J. Am. Chem. Soc.* **1996**, *118*, 6317; b) Z. Chen, C. S. Wannere, C. Corminboeuf, P. v. R. Schleyer, *Chem. Rev.* **2005**, *105*, 3842.
[12] K. B. Wiberg, *Tetrahedron* **1968**, *24*, 1083.
[13] A. Haaland, *Acc. Chem. Res.* **1979**, *12*, 415.
[14] S.-D. Li, J.-C. Guo, C.-Q. Miao, G.-M. Ren, *Angew. Chem. Int. Ed.* **2005**, *44*, 2158.

Received: October 2, 2007
Published Online: January 17, 2008

